

ELASTIC ELECTRON SCATTERING BY Pb^{208} AND
NEW INFORMATION ABOUT THE NUCLEAR CHARGE DISTRIBUTION*

J. Heisenberg,† R. Hofstadter, J. S. McCarthy, and I. Sick

Department of Physics and High Energy Physics Laboratory, Stanford University, Stanford, California 94305

and

B. C. Clark and R. Herman

General Motors Research Laboratories, Warren, Michigan 48090

and

D. G. Ravenhall

Physics Department, University of Illinois, Urbana, Illinois 61801

(Received 17 October 1969)

An analysis of electron-scattering experiments gives a nuclear charge distribution which (A) has a central depression of about 7%, (B) falls off at the nuclear edge faster than the customarily used Fermi distributions, (C) has no detectable energy dependence, and (D) appears to have an undulation of rather small magnitude.

New experiments are reported on the scattering of 248.2- and 502.0-MeV electrons by Pb^{208} . Partial-wave analyses of the differential cross sections in terms of a static nuclear charge distribution $\rho(r)$ give direct evidence of the following nuclear characteristics. (A) The shape we find for $\rho(r)$ by fitting the low- q part of the data, which is a smoothed average of the actual charge distribution, has a central depression, $1-\rho(0)/\rho_{\text{max}}$, of about 7%. (B) The extreme edge of $\rho(r)$ falls off with a different dependence on r than has been assumed in previous analyses. (C) Close agreement between the results obtained at the two experimental energies limits very strongly any possible energy dependence in $\rho(r)$. (D) The high- q part of the cross sections shows a structure similar to that of earlier calcium experiments,¹ which were analyzed in terms of an additional undulation in $\rho(r)$. Preliminary analyses of this feature for Pb^{208} are presented. We also discuss the connection between these new observations and nuclear models.

As regards earlier work, the present 250-MeV experimental results have improved accuracy and extend further in angle than earlier measurements of Bellicard and van Oostrum.² An analysis³ of those data² in combination with Pb^{208} muonic x-ray energies has already given evidence for the central depression,⁴ although it was hardly detectable in the electron data as analyzed in Ref. 2. The depression has been commented on also by Bethe and Elton.⁵

Experimental facilities have been described in a recent paper.⁶ We mention only the new features essential for the higher accuracy of the

present data. A nuclear magnetic resonance probe used to measure the field in the deflecting magnet has been calibrated by a floating wire method.⁷ The accuracy obtained for the energy is better than $\pm 0.1\%$ and the reproducibility is about $\pm 0.05\%$. A retractable screen 5 m upstream from the target allows the direction of the incoming beam to be adjusted to $(0.00 \pm 0.02)^\circ$. The amplified signal of a split secondary-emission monitor (SEM) regulates the current of a pair of Helmholtz steering coils and stabilizes the beam position to ± 0.5 mm, thus keeping the scattering angle constant. A second SEM upstream from the target measures the beam current at scattering angles smaller than 32° . The scattering angle has been recalibrated to $\pm 0.03^\circ$. An increase in the beam current by a factor two to four produces better statistics at smaller cross sections.

The approach employed in analyzing these experiments is similar to that in our Ca isotope work.⁶ In the static nuclear charge distribution $\rho(r)$ which we fit to the data by means of a partial-wave analysis, we search for characteristics which are independent of the method of fitting and of the assumed functional form for $\rho(r)$. For this purpose we have used the shapes

$$\rho_1(r) = \rho_0 [1 + w r^2 / c^2] f_{c,z,n}(r), \quad (1)$$

where

$$f_{c,z,n}(r) = \{1 + \exp[(r^n - c^n)/z^n]\}^{-1}, \quad (1a)$$

$$\rho_2(r) = \rho_0 [f_{c,z,n}(r) + w(r^2/c^2)f_{c,z,n}^2(r)], \quad (2)$$

and

$$\rho_3(r) = \rho_0 [1 + wr^2/c^2] [f_{c,z,n}(r)]^n. \quad (3)$$

The form (2) differs from (1) and (3) in that it confines the central depression, governed by w , to the central regions, and does not allow it to affect the edge of the charge distribution. The parameter n allows the extreme edge of the distribution to fall off at a rate independent of the surface behavior, governed by z . The form (3) grew out of shapes suggested to us by Myers and Swiatecki,⁸ who wished to avoid a surface symmetrical about its midpoint. This nonsymmetry is also a property of (1) and (2). The values obtained for c , z , w , and n by the fitting procedure are quite different for ρ_1 , ρ_2 , and ρ_3 , but the actual shape obtained for $\rho(r)$ is the same. The central depression and the more rapid fall-off at the extreme edge are, we believe, representative of the data and not only of a particular parametrization.

Some of our results are obtained by making a simultaneous fit to muonic x-ray energies.⁹ These energies provide in the K_α and L_α lines two experimental numbers which enable us to fix two of our adjustable parameters, and thus extract more accurate information about the remaining parameters in $\rho(r)$ from the electron scattering.¹⁰ The evidence from earlier work

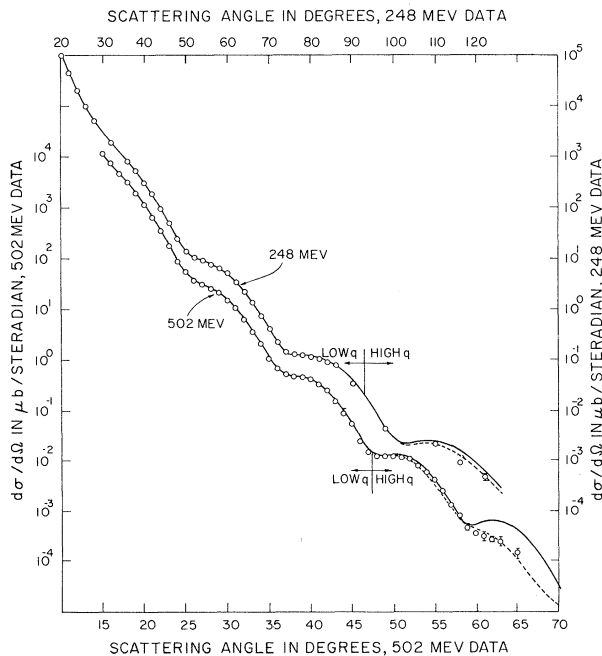


FIG. 1. Experimental cross sections for 248.2- and 502.0-MeV electrons scattered by Pb^{208} , and theoretical cross sections obtained with shape (1), using parameter values given in the top line of Table I.

with the calcium isotopes,⁶ and new Ca^{40} results,¹¹ provide partial justification for combining muonic x-ray and electron-scattering experiments when examining lead. We also make analyses of our data without use of the muonic x-ray energies. The central depression persists, and the edge fall-off is also present to some extent. This is not in accord with the view expressed by Bethe and Elton⁵ on the accessibility of information about $\rho(r)$.

In Fig. 1 are shown the experimental data and our fit to them. The full curve in Fig. 2 shows a plot of $\rho(r)$. The curves we obtain for $\rho(r)$ are identical, to the accuracy of a drawing, for each of the assumed forms ρ_1 , ρ_2 , and ρ_3 . In the region of the surface, the shape resembles closely earlier results on heavy nuclei.¹² Defining a surface thickness t' as the distance over which $\rho(r)$ falls from 90 to 10% of its maximum value, we obtain $t' = 2.37$ F, compared with the earlier result for Au^{197} , $t = 2.32$ F. Analyses of muonic x-ray data in terms of Fermi distributions, shape (1) with $w = 0$, $n = 1$ (see, e.g., Ref. 9), produce smaller surface thicknesses. Such shapes would give completely unacceptable fits to our data. To obtain fits to all of the data, muon and electron, the central depression seems to us essential.

Parameter values and r_{rms} are given in Table I, with results of earlier analyses.^{2,3} We note the general agreement. The rms radius of our combined $e + \mu$ fit, $r_{rms} = 5.501$ F, is in agreement with the value obtained in Anderson and co-

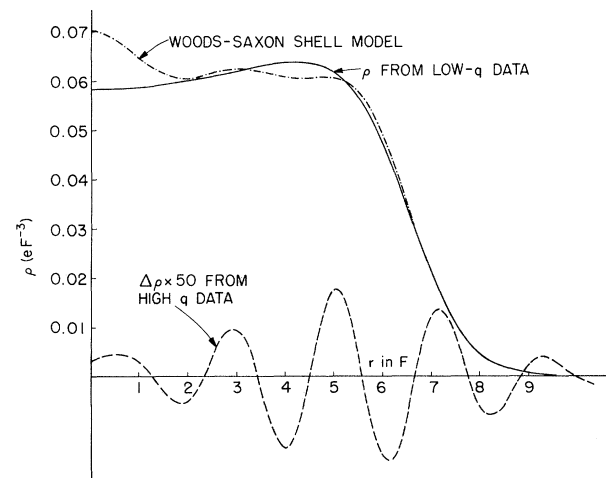


FIG. 2. The charge distribution of Pb^{208} (full curve). It represents all three of our $e + \mu$ fits given in Table I. The dashed curve shows $\Delta\rho(r) \times 50$. The dash-dot curve is a typical shell-model charge distribution (see text).

Table I. Values for the adjustable parameters in the shapes (1), (2), and (3) obtained from either a mutual fit to our 248.2 MeV results and to the muonic K_{α} and L_{α} x-ray energies of Anderson, Ref. 9, or a fit to our data alone, as indicated in the second column. Errors, where given, indicate a rough range of variation, but because of strong error correlations they cannot be used individually to obtain the error in $\rho(r)$. For the same reason, parameter values are given to more precision than that to which each can be determined independently. Also given are results of the earlier work of Refs. 2 and 3.

Shape	Method	c in F	z in F	w	n	r_{rms} in F
1	e+ μ	6.3032	2.8882	0.3379(± 0.05)	2.0(± 0.2)	5.501
1	e alone	6.2773	2.9110	0.4345	2 ^a	5.535
2	e+ μ	6.4745	2.975	0.361	2 ^a	5.502
2	e alone	6.4831	3.0319	0.4909	2 ^a	5.539
3	e+ μ	6.7503	0.7000	0.315	1.5(± 0.1)	5.501
3	e alone	6.7223	0.7219	0.4443	1.5 ^a	5.546
1	e alone Ref. 2	6.40 \pm .06	0.542 \pm .009	0.14 \pm .10	1 ^a	5.42
1	e+ μ Ref. 3 ^b	6.40	0.540	0.32	1 ^a	5.490
1	e+ μ Ref. 3 ^b	6.34	2.85	0.32	2 ^a	5.492

^a Assumed, not fitted.

^b Muonic x-ray data of Backenstoss and co-workers (see Ref. 4), with natural Pb.

workers' muonic x-ray study,⁹ $r_{rms} = (5.4978 \pm 0.0030)$ F. The values obtained from our electron scattering alone center around $r_{rms} = 5.54$ F. With this difference, 0.04 F, taken as a measure of our error, our result overlaps the value obtained by van Niftrik¹³ from low-energy electron scattering, $r_{rms} = (5.46 \pm 0.06)$ F.

Our search for a possible energy dependence of $\rho(r)$ has used two methods. One is to compare parameter values, and $\rho(r)$, obtained by fitting separately at the two energies. The other is to take the $\rho(r)$ obtained from the lower energy and calculate the electron energy at which it best fits the data at the higher energy. In either method we consider the same range of the recoil momentum q corresponding to the angular ranges $\theta \leq 90^\circ$ at 250 MeV, $\theta \leq 46^\circ$ at 500 MeV. In both cases the agreement is within the error limits. In the latter case the energy we find is 502.1 MeV, compared with the measured value (502.0 \pm 0.5) MeV. We conclude that at this new level of precision, there is no detectable energy dependence in $\rho(r)$.¹⁴

Investigation of the irregularity in the struc-

ture of the 502.0-MeV cross section starting at $\theta \approx 46^\circ$ proves to be more difficult than in the corresponding Ca analysis.¹ We use a form-factor approach as a guide to the manner in which $\rho(r)$ must be modified. In Pb, it is a poorer guide because of the greater distortion of the electron wave fronts. The dashed curve shown in Fig. 1 is the best fit we have achieved. It is obtained by adding to the smooth charge distribution $\rho(r)$ a small undulation $\Delta\rho(r)$ whose form is shown as the dashed curve in Fig. 2.

Some comparisons have been made with the independent-particle shell model.¹⁵ The fall-off of $\rho(r)$ at the edge of the nucleus, which we now find is more rapid than can be described by a single exponential, is well described by that model. It occurs because the tails of the deeper proton orbitals drop off with increasing rapidity, due to their greater binding energy. On the other hand, the central depression of $\rho(r)$ would appear from Fig. 2 to be in qualitative disagreement with the average trend of the shell-model charge density, for which a typical shape¹⁶ is also shown.¹⁷ The undulation has about the same wavelength and

phase as the wiggle on the shell-model charge distribution. It seems to be considerably smaller in magnitude than that obtained from the shell model, as is evident from Fig. 2. This diminution of the shell-model undulation, attributed in Ca⁴⁰ and Ca⁴⁸ to the effect of nuclear correlations,¹⁸ appears to be much more pronounced in Pb²⁰⁸. Details of this last result are preliminary, however, and we are searching for a better fit to the high- q data. A quantitative analysis of the data directly in terms of the shell-model is also in progress.¹⁵

We observe that the shell model and Hartree-Fock calculations,¹⁹ which are independent-particle models and which therefore ignore long-range correlations, both have no central depression and have too large an undulation. A semi-classical model, which includes long-range correlations, apparently can give a charge density with a central depression.^{5,20} We surmise that the central depression and the much diminished undulation are both pieces of evidence for strong correlations in the nucleus Pb²⁰⁸.

*Work supported in part by the National Science Foundation.

†Work supported in part by the Bundesministerium für Wissenschaft und Forschung, Germany.

¹J. B. Bellicard *et al.*, Phys. Rev. Letters **19**, 527 (1967), and **20**, 977 (E) (1968).

²J. B. Bellicard and K. J. van Oostrum, Phys. Rev. Letters **19**, 242 (1967).

³See B. C. Clark *et al.*, in Proceedings of the International Conference on Electromagnetic Sizes of Nuclei, Ottawa, Canada, 22-27 May 1967, edited by D. J. Brown, M. K. Sundaresan, and R. D. Barton (Carleton University Press, Ottawa, Canada, 1968), p. 129.

⁴Qualitatively the same result was also perceptible in early Au¹⁹⁷ data [B. Hahn *et al.*, Phys. Rev. **101**, 1131 (1956)] when analyzed together with muonic x-ray measurements [H. L. Acker *et al.*, Nucl. Phys. **87**, 1 (1966)]; D. G. Ravenhall, B. C. Clark, and R. Herman, to be published.

⁵H. A. Bethe and L. R. B. Elton, Phys. Rev. Letters **20**, 745 (1968).

⁶R. F. Frosch *et al.*, Phys. Rev. **174**, 1380 (1968).

⁷J. Heisenberg *et al.*, High Energy Physics Laboratory, Stanford University, Internal Report No. TN-68-16, 1968 (unpublished).

⁸W. D. Myers and W. J. Swiatecki, private communications.

⁹H. L. Anderson *et al.*, Phys. Rev. Letters **22**, 221 (1969), and Phys. Rev. (to be published).

¹⁰Included in the muon Hamiltonian for the energy-level calculations is an improved approximation to the second-order vacuum polarization [J. M. McKinley and D. G. Ravenhall, Bull. Am. Phys. Soc. **14**, 88 (1969), and Phys. Rev. (to be published)]. The Lamb shift [see R. C. Barrett *et al.*, Phys. Rev. **166**, 1589 (1968)] and nuclear polarization [see, e.g., R. K. Cole, Jr., Phys. Rev. **177**, 164 (1969)] are not included. These effects tend to cancel each other, and in any case are unimportant compared with the accuracy level of the electron-scattering analysis. One of us (D.G.R.) acknowledges many helpful discussions with Dr. McKinley on these matters.

¹¹Present authors, to be published.

¹²Hahn *et al.*, see Ref. 4.

¹³C. J. C. van Niftrik, Nucl. Phys. **A131**, 574 (1969).

¹⁴As was observed in Ref. 7, Sec. V, present calculations of the effect of nuclear polarization on electron scattering, as reported in the references cited there, show results which are to a good approximation dependent only on q , the recoil momentum, and not on the energy at a fixed q .

¹⁵See, for example, A. Swift and L. R. B. Elton, Phys. Rev. Letters **17**, 484 (1966); Bethe and Elton, Ref. 5. The particular results reported here are obtained by L. R. Mather, R. H. Landau, and D. G. Ravenhall, to be published.

¹⁶With a Woods-Saxon central potential $V(r) = V_0 \times \{\exp[(r-r_0A^{1/3})/a] + 1\}^{-1}$ and a spin-orbit potential $V_{so}(r) = \lambda\sigma \cdot L(\hbar/2m_p c)^2(1/r)\partial V(r)/\partial r$ having the same parameters as $V(r)$, the values used to obtain this charge distribution are $V = 57$ MeV, $r_0 = 1.26$ F, $a = 0.70$ F, and $\lambda = 37.2$. Finite proton size is allowed for.

¹⁷The shape given by Bethe and Elton, Ref. 5, Fig. 1, displays similar characteristics to ours. The peaking at the center that they show is somewhat larger.

¹⁸This was originally suggested to one of us (D.G.R.) by M. Baranger. Inclusion of two-nucleon correlations in Ca⁴⁰ has been considered by F. C. Khanna, Phys. Rev. Letters **20**, 871 (1968); and in $1p$ -shell nuclei by C. Ciofi degli Atti, Nucl. Phys. **A129**, 350 (1969); S. T. Tuan, L. E. Wright, and M. G. Huber, Phys. Rev. Letters **23**, 174 (1969).

¹⁹See, for example, R. M. Tarbuton and K. T. R. Davies, Nucl. Phys. **A120**, 1 (1968); D. Vautherin and M. Veneroni, Phys. Letters **29B**, 203 (1969).

²⁰R. Mohan, M. Danos, and L. C. Biedenharn, Phys. Rev. Letters **23**, 868 (1969).